Size and Temperature Dependence of the Plasmon Absorption of Colloidal Gold Nanoparticles

Stephan Link and Mostafa A. El-Sayed*

Laser Dynamics Laboratory, Georgia Institute of Technology, School of Chemistry and Biochemistry, Atlanta, Georgia 30332-0400

Received: December 18, 1998; In Final Form: April 2, 1999

The size and temperature dependence of the plasmon absorption is studied for 9, 15, 22, 48, and 99 nm gold nanoparticles in aqueous solution. The plasmon bandwidth is found to follow the predicted behavior as it increases with decreasing size in the intrinsic size region (mean diameter smaller than 25 nm), and also increases with increasing size in the extrinsic size region (mean diameter larger than 25 nm). Because of this pronounced size effect a homogeneous size distribution and therefore a homogeneous broadening of the plasmon band is concluded for all the prepared gold nanoparticle samples. By applying a simple two-level model the dephasing time of the coherent plasmon oscillation is calculated and found to be less than 5 fs. Furthermore, the temperature dependence of the plasmon absorption is examined. A small temperature effect is observed. This is consistent with the fact that the dominant electronic dephasing mechanism involves electron−electron interactions rather than electron−phonon coupling.

Introduction

The electronic and optical properties of nanoparticles are determined by both their size and shape.[1−13] Metal nanoparticles have mainly been studied because of their unique optical properties.[5−12] Nanoparticle colloidal solutions of the noble metals copper, silver, and gold show a very intense color, which is absent in the bulk material as well as for the individual atoms. Their origin is attributed to the collective oscillation of the free conduction electrons induced by an interacting electromagnetic field.[5,6,9,10] These resonances are also denoted as surface plasmons. Mie[14] was the first to describe them quantitatively by solving Maxwell's equations with the appropriate boundary conditions for spherical particles. The total extinction cross section composed of absorption and scattering is given as a summation over all electric and magnetic multipole oscillations. The Mie theory has the advantage of being conceptually simple and has found wide applicability in explaining experimental results.[5,6]

For nanoparticles small compared to the wavelength λ of the exciting light ($\lambda \gg 2R$, for gold $2R < 25$ nm [5]) only the dipole absorption of the Mie equation contributes to the extinction cross section σ_{ext} of the nanoparticles. The Mie theory then reduces to the following relationship (quasi-static or dipole approximation):[6,9−11]

$$\sigma_{ext} = \frac{9V\epsilon_m^{3/2}}{c} \cdot \frac{\omega\epsilon_2(\omega)}{[\epsilon_1(\omega) + 2\epsilon_m]^2 + \epsilon_2(\omega 2)^2} \qquad (1)$$

where V is the spherical particle volume, c the speed of light, ω the angular frequency of the exciting radiation, and ϵ_m is the dielectric constant of the surrounding medium (assumed to be frequency independent). $\epsilon_1(\omega)$ and $\epsilon_2(\omega)$ denote the real and imaginary part of the dielectric function of the particle material, respectively ($\epsilon(\omega) = \epsilon_1(\omega) + i\epsilon_2(\omega)$).

From eq 1 it follows that resonance occurs when $\epsilon_1(\omega) \approx -2\epsilon_m$ if ϵ_2 is small or only weakly dependent on ω. The bandwidth and peak height are roughly determined by $\epsilon_2(\omega)$.[5] However, within the dipole approximation there is no size dependence except for a varying intensity due to the fact that the volume V depends on the particle radius R. Experimentally, one however observes a strong size dependence of the plasmon bandwidth.[15] The position of the absorption maximum is also affected although both a blueshift and a red-shift have been observed with decreasing particle size.[15] As a modification to the Mie theory for small particles, the dielectric function of the metal nanoparticles itself is assumed to become size dependent [$\epsilon = \epsilon(\omega, R)$] and therefore rendering a size-dependent absorption cross section even within the dipole approximation (intrinsic size effects).[5]

The size dependence of the dielectric constant is introduced as the diameter of the particle becomes smaller than the mean free path (MFP) of the conduction electrons. This classical picture of the limitation of the MFP due to surface scattering has been suggested by Kreibig and results in a $1/R$ dependence of the plasmon bandwidth, in agreement with experimental results.[16] In a quantum mechanical model, Kawabata and Kubo[17] argue that the surface does not act as a scatterer but mainly determines the energy eigenstates of the system and that the decay or damping of the plasmon absorption is caused by transfer of its energy to the excitation of individual electronic states. They also calculate for the plasmon bandwidth in the quasi-static limit to follow a $1/R$ law.

A $1/R$ dependence of the plasmon bandwidth is furthermore predicted by a more recent quantum mechanical theory by Persson[18] considering the chemical nature of the nanoparticle-surrounding interface. Following this model, an additional broadening of the plasmon band is caused by the transfer of the excitation energy into adsorbate levels located above the Fermi level. This model is therefore called chemical interface damping and excellent quantitative agreement was found by Kreibig and co-workers[19,20] by measuring the same 2 nm silver

* Author to whom correspondence should be addressed.

10.1021/jp984796o CCC: $18.00 © 1999 American Chemical Society
Published on Web 05/07/1999

nanoparticles in a vacuum (naked clusters), supported on and embedded into a SiO_2 matrix. Chemical interface effects could thus be isolated from size effects.

For larger nanoparticles ($2R > 25$ nm) the extinction cross section is also dependent on higher-order multipole modes within the full Mie equation and the extinction spectrum is then also dominated by quadrupole and octopole absorption as well as scattering.[6,9−11] These higher oscillation modes explicitly depend on the particle size and with increasing size the plasmon absorption maximum is shifted to longer wavelength and the bandwidth increases. The total plasmon band absorption is then the superposition of all contributing multipole oscillations peaking at different energies. The excitation of the higher-order modes is explained in terms of an inhomogeneous polarization of the nanoparticles by the electromagnetic field as the particle size becomes comparable to the wavelength of the exciting radiation. The broadening of the plasmon band is then usually ascribed to retardation effects.[5] On the other hand, the increased line width or equivalently the faster loss of coherence of the plasmon resonance could qualitatively also be described as a result of the interactions between the dipole and the quadrupole (and higher-order) oscillatory motions of the electrons, thus destroying the phase coherence. As the size effect enters through the full Mie equation and the complex dielectric function of the bulk material, which is no longer size dependent, is used, this behavior of the plasmon resonance is regarded as an extrinsic size effect.[5]

The size effect on the plasmon absorption is examined in this letter by studying colloidal gold nanoparticles with an average diameter between 9 and 99 nm, thus covering both intrinsic and extrinsic size effects. The plasmon bandwidth is found to follow the predicted behavior and, therefore, a homogeneous size distribution is concluded for all the prepared gold nanoparticle samples. By applying a simple two-level model, the dephasing time of the coherent plasmon oscillation is calculated and found to be less than 5 fs. Furthermore, the temperature dependence of the plasmon absorption is examined. Only a small temperature effect is observed, which is consistent with the fact that dephasing of the surface plasmon electron motion is a result of electron−electron repulsion rather than electron−phonon interaction.

Experimental Section

The colloidal gold nanoparticles are prepared following a method introduced by Turkevich.[21] A volume of 95 mL of a chlorauric acid ($HAuCl_4$) solution containing 5 mg of Au are refluxed and 5 mL of 1% sodium citrate solution is added to the boiling solution. The reduction of the gold ions by the citrate ions is complete after 5 min while the solution is further boiled for 30 min and is then left to cool to room temperature. This method yields spherical particles with an average diameter of about 20 nm. Although the actual value of the mean size might vary slightly from each preparation, the size distribution is found to be always about 10% standard deviation.

Larger particles are produced by the reduction of $HAuCl_4$ with hydroxylamine hydrochloride in the presence of already existing gold nanoparticles from the preparation described above.[22] As the reducing agent hydroxylamine hydrochloride cannot act as a nucleating but only as a growth agent in slightly acidic conditions, the particle size of the existing particles is steadily increased. The 20 nm particles therefore form the nuclei of the larger ones. The size of the final particles is simply given by the amount of $HAuCl_4$ used. A quantitative formula that allows one to estimate the final particle size is given by Turkevich.[23]

Gold nanoparticles with an average diameter of about 10 nm are prepared by reversing the order of addition of gold salt and sodium citrate.[24] This means that in our preparation 68 mg of sodium citrate in 105 mL water are boiled and then 1 mL of aqueous solution containing 9.5 mg $HAuCl_4$ is added. Boiling is then continued for 15 min.

The size of the particles is analyzed by transmission electron microscopy (TEM) using a Hitachi HF-2000 field emission TEM operating at 200 kV. From the TEM images the size distributions of the different samples are determined by counting at least 300 particles. The UV−vis absorption spectra are recorded on a Beckman DU 650 spectrophotometer in a 1 cm glass cuvette. The temperature is controlled by a thermostat (Neslab RTE−100).

Results

Gold nanoparticles with average diameters of 9, 15, 22, 48, and 99 nm are prepared as described above. TEM images of the 22, 48, and 99 nm gold nanoparticles are shown in Figure 1, parts a, b, and c, respectively. The nanoparticles' shape is nearly spherical. The statistical analysis of the particles for all samples reveals a size distribution of about 10% mean standard deviation σ, defined as $\sigma = ((1/N\,(N-1)) \times \Sigma_i\,(x_i - x)^2)^{1/2}$. The size histograms of the 22, 48, and 99 nm gold particles corresponding to the TEM pictures are given in parts d, e, and f of Figure 1, respectively.

Table 1 summarizes the data of all five samples. The particle diameter and the mean standard deviation as well as the plasmon bandwidth and its maximum are given (see Figure 2 below). The width is determined by assuming a symmetric plasmon band (in the free electron limit the plasmon band should be a Lorentzian curve). The width is then measured as twice the distance from the low-energy side of the absorption band to the maximum position at half the maximum intensity.

Figure 2a shows the absorption spectra of four different size gold nanoparticles. The plasmon absorption is clearly visible and its maximum red-shifts with increasing particle diameter ($\lambda_{max} = 517$, 521, 533, and 575 nm for the 9, 22, 48, and 99 nm particles). In Figure 2b the dependence of the plasmon bandwidth is plotted against the particle diameter. From this plot it can be seen that the width first decreases with increasing particle size and then increases again with a minimum for the 22 nm nanoparticles.

In Figure 3 the absorption spectra for the 22 nm gold nanoparticles at 18 and 72 °C are shown. The temperature effect is very small, resulting in just a decrease in intensity of the maximum while a broadening of the plasmon band is not visible. Furthermore, the maximum of the plasmon absorption remains unchanged. Similar results are obtained for the other sizes.

Discussion

The statistical analysis of the particles for all samples reveals a size distribution of about 10%. The nearly constant mean standard deviation means that the width of the different samples can very well be compared with each other. The size distribution of the individual samples therefore does not obscure the predicted behavior for the plasmon bandwidth. Furthermore, as the bandwidth does vary with size as predicted (Figure 2), this strongly suggests that the width is not inhomogeneously broadened due to a 10% size distribution. For comparison, the size distribution for the small silver particles grown in glass matrixes, from which the $1/R$ dependence was deduced experimentally, was stated as 74% of the particles having radii between

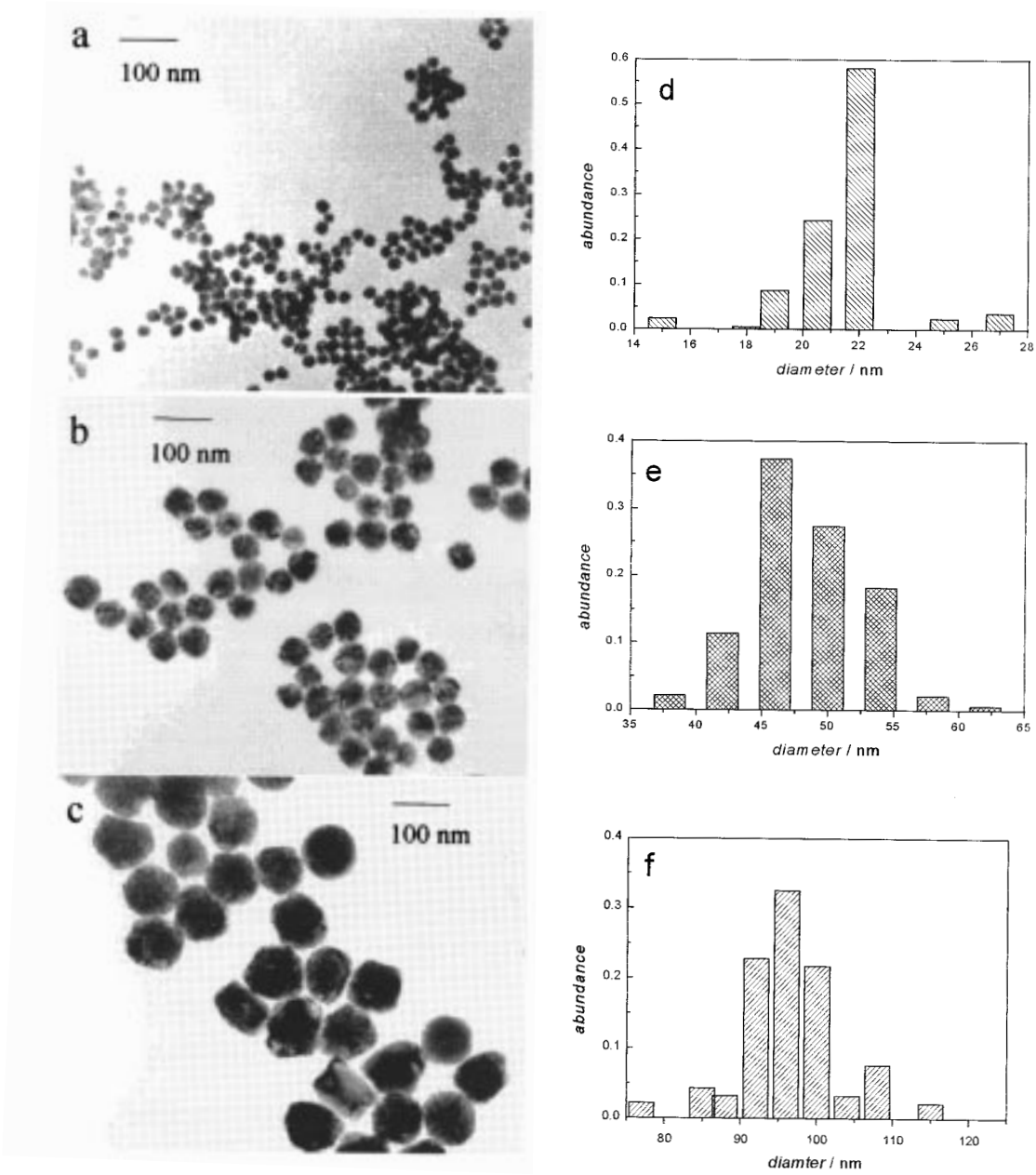

Figure 1. TEM images of the 22 (a), 48 (b), and 99 nm (c) gold nanoparticles corresponding to the absorption spectra in Figure 2. The corresponding size histograms are given in parts d−f, respectively. The mean sizes and size distributions of all 5 samples are also summarized in Table 1.

TABLE 1: Summary of the Size and Size Distribution of the Gold Nanoparticles[a]

diameter [nm]	mean standard deviation [%]	λ_{max} [nm]	Γ [eV]	T_2 [fs]
8.9	13	517	0.42	3.1
14.8	12	520	0.34	3.9
21.7	9	521	0.32	4.1
48.3	11	533	0.34	3.9
99.3	11	575	0.50	2.6

[a] The position of the plasmon band maximum and its width are also included; the total dephasing time T_2 has been calculated with eq 5.

$0.7 < R_i/R < 1.3$ (R is the mean radius).[25] The 11% size distribution for the 48 nm particles corresponds to *all* the particles falling in that size range. In fact, 65% of the 48 nm particles have radii between $0.9 < R_i/R < 1.1$. A homogeneous line broadening is therefore also assumed for these larger gold nanoparticles. It was often argued that larger colloids grown rapidly in water have an inhomogeneous size distribution as an obvious size and temperature dependence were not observed.[8,26]

The major drawback of the Mie theory and its modifications for the intrinsic size effects is, however, that the underlying relaxation mechanisms are all included by the macroscopic material dielectric function, which does not distinguish between several possible decay processes. These decay mechanisms of the coherent motion of the free electrons include both energy and momentum (dephasing of the collective electron motion[27]) dissipation and are directly related to the width of the plasmon resonance. A microscopic picture for the plasmon absorption is therefore lacking within the Mie theory.

For a free electron gas the intraband contribution to the dielectric function can be written within the Drude−Sommerfeld model as[16,28]

$$\epsilon(\omega) = 1 - \frac{{\omega_p}^2}{\omega^2 + i\gamma\cdot\omega} \qquad (2)$$

The plasmon frequency ${\omega_p}^2 = (n\, e^2/\epsilon_0 m_{eff})$ depends on the electron density n and on the electron effective mass m_{eff}. e is

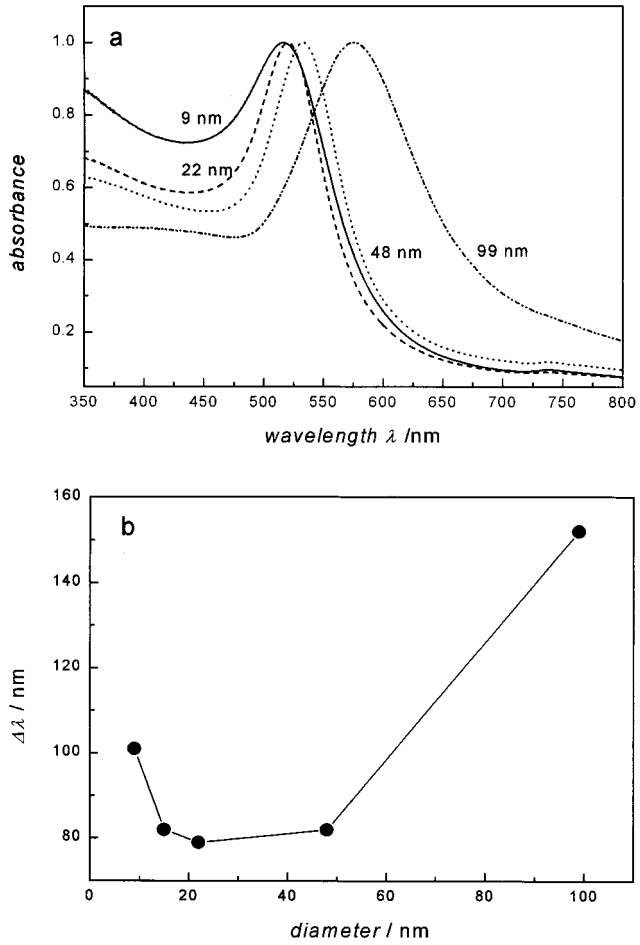

Figure 2. (a) UV−vis absorption spectra of 9, 22, 48, and 99 nm gold nanoparticles in water. All spectra are normalized at their absorption maxima, which are 517, 521, 533, and 575 nm, respectively. (b) The plasmon bandwidth $\Delta\lambda$ as a function of particle diameter.

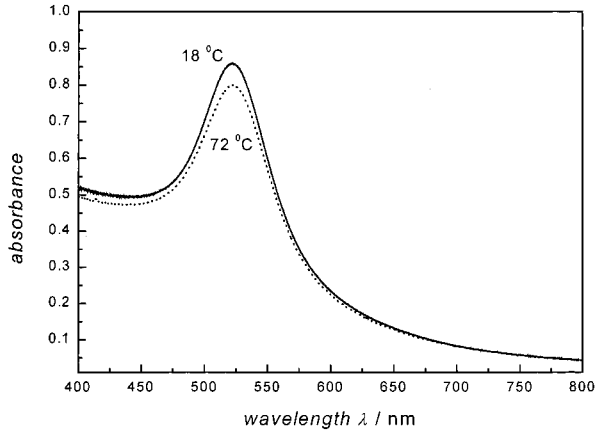

Figure 3. Temperature dependence of the plasmon band absorption for the 22 nm gold nanoparticles. The absorption spectra are measured at 18 °C (solid line) and 72 °C (dashed line).

the electron charge and ϵ_0 the vacuum permittivity. γ is the phenomenological damping constant of the bulk material. In the case of a perfectly free electron gas and in the limit of $\gamma \ll \omega$, the width Γ of the plasmon band is given by the damping constant γ while for realistic metals the width takes a more complex function being dependent on the full expression for the real and imaginary parts of the dielectric function consisting of an intraband and an interband term.[5]

For a bulk metal with infinite boundaries the damping constant γ is determined by electron−electron, electron−phonon, and electron-defect scattering processes, where the last term usually includes grain boundaries, impurities, and dislocations. γ is therefore closely related to the electrical resistivity of the metal and one can express γ as the sum over all reciprocal relaxation times τ:[5]

$$\gamma = \sum_i (\tau_i)^{-1} = (\tau_{e-e})^{-1} + (\tau_{e-ph})^{-1} + (\tau_{e-d})^{-1} \qquad (3)$$

For the bulk the electron−phonon term is the dominating one, and furthermore γ should be a constant. However, for small particles this is assumed not to be valid. The surface acts as an additional scatterer because the mean free path of the electrons becomes comparable to the size of the particles (Drude−Sommerfeld model of a free electron gas: MFP in gold is about 50 nm with an electron−phonon collision time of 35 fs.[29,30]) For very small particles these interactions (collisions) of the conduction electrons with the particle surface dominate and this results in a reduced effective MFP. According to this model, the damping constant γ then depends on the particle radius R:[16]

$$\gamma(R) = \gamma_0 + \frac{A \cdot v_F}{R} \qquad (4)$$

γ_0 is the bulk damping constant as given by eq 3. v_F is the velocity of the conduction electrons at the Fermi energy, and A includes details of the scattering processes.[15]

Although this model gives a better physical understanding about the plasmon absorption, especially for the intrinsic size effects, it is still based on ideas from solid-state physics. However, if one assumes a simple two-level model for the plasmon absorption as in molecular spectroscopy the width is then given by[27]

$$\frac{1}{T_2} = \pi c \Gamma = \frac{1}{2 \cdot T_1} + \frac{1}{T_2^*} \qquad (5)$$

T_1 describes the population relaxation time (radiative and nonradiative processes) and T_2 is the total dephasing time or resonance damping constant. T_2* is the pure dephasing time which may originate from collisions that change the plasmon wave vector but not its energy. Often T_2* is much shorter than the energy relaxation T_1 and thus determines the value of T_2.

Assuming a homogeneous size distribution and therefore homogeneous line broadening, the total dephasing time can be computed from the measured width of the plasmon bands in Figure 2 using eq 5. The calculated values are given in Table 1 for the five different nanoparticle samples. The dephasing times all lie in the range of a few femtoseconds. These extremely fast dephasing times are in agreement with nonlinear frequency mixing studies of Hochstrasser et al. on gold nanoparticles who found that both T_1 and T_2 are shorter than 48 fs.[27] Furthermore, other more recent nonlinear studies come to the conclusion that the dephasing time of the coherent plasmon oscillation is shorter than 20 fs.[31] These results also agree with studies on lithographically produced 200 nm silver nanoparticles[32] and evaporated silver island films[33] (20 nm island size), for which dephasing times of 10 and 40 fs were measured. Furthermore, Kreibig et al.[20] determined dephasing times of 2 and 7 fs for 2 nm silver clusters embedded in a matrix and in a vacuum (naked clusters) from the width of the plasmon band.

Recent single nanoparticle investigations with a scanning near-field optical microscope (SNOM) found a homogeneous line width of only 160 meV for some individual particles corresponding to a dephasing time of 8 fs for 40 nm gold

nanoparticles in a sol−gel TiO_2 matrix.[34] The ensemble line width for this sample was 300 meV. The assumption above that the plasmon band for our samples is homogeneously broadened should then be incorrect. However, other nanoparticles of the sample investigated by SNOM show a bandwidth comparable to the total ensemble line width. This is explained by imperfections of the nanoparticle−matrix interface leading to a variation in the plasmon bandwidth due to chemical interface damping. The fact that interface effects are of comparable if not larger influence than size effects[19,20] and that nevertheless a size dependence is observed for the colloidal solution in Figure 2 leads to the conclusion that the magnitude of an additional broadening caused by the citrate ions adsorbed at the nanoparticle surface is of the same order for all samples in this study. Judging from the synthesis procedure, this is chemically justified, as citrate ions are present in excess for all sizes and a dynamical equilibrium between adsorbed and free citrate ions in solutions is expected thus averaging out any interface imperfections. However, to solve this remaining question of a homogeneous plasmon band broadening experimentally we are working on measuring the dephasing time of these nanoparticle samples directly by a frequency-resolved optical gating technique analogous to the method used for characterization of ultrashort laser pulses (FROG). By adding other substances to the gold nanoparticle surface we further hope to compare the effect of chemical interface damping on the plasmon bandwidth with the measured dephasing time.

Examining the temperature dependence of the plasmon absorption might give some further insight regarding which scattering process dominates the dephasing of the coherent electron motion. Kreibig has evaluated the temperature dependence of small silver and gold clusters (diameters of 1 to 10 nm) in a glass matrix and found that the spectrum decreases in intensity and broadens when increasing the temperature from 1.5 to 300 K.[25,35,36] Kreibig explained his results on the size dependence of the temperature dependence of the Mie resonance of gold nanoparticles in terms of two effects. The temperature dependence of the electron−phonon scattering is partially compensated by a thermal lattice contraction of the nanoparticles with decreasing temperature. The latter becomes more pronounced with decreasing nanoparticle size. In addition, changes of the band structure in nanoparticles below 5 nm are assumed to be effective.[5]

Doremus investigated gold nanoparticles of 12 nm diameter in a glass matrix and varied the temperature from 196 to 514 °C.[37,38] He also found a broadening of the plasmon band accompanied with a decrease in intensity and a slight red-shift of the maximum. The observed changes over such a wide temperature range are, however, much smaller than expected. Doremus' explanation was that the electron concentration n, which determines the plasmon frequency, is decreased with increasing temperature and therefore changes the overall absorption spectrum. This is the same as considering a lattice expansion as the electron density can otherwise change only if the particles become charged.

The small temperature dependence found for the 22 nm gold nanoparticles in Figure 3 is consistent with the studies by Kreibig and Doremus who examined a much wider temperature range. No temperature dependence of the plasmon bandwidth is also found for the other sizes. It can be concluded that the temperature has to be raised by several hundred degrees in order to record a significant line broadening. This is of course not possible without changing from water to an inert matrix. As the refractive index of the water also changes with temperature it causes a decrease in intensity and a blue shift as well as a decrease in the plasmon bandwidth. The last two changes are opposite to the ones expected from changes due to the heating of particles themselves and could obscure the anticipated changes.

Considering the different interactions already mentioned above—electron−electron, electron−phonon, electron-defect, and surface scattering—a small temperature dependence of the bandwidth is in contrast with a strong electron−phonon coupling being responsible for the loss of the coherence as this process is normally strongly temperature dependent. In molecules or very small clusters higher vibrational states have to be excited thermally in order to couple with the electronic states and their large amount of energy compared to the vibrational quanta.[39] This does not rule out that subsequent energy relaxation due to electron−phonon coupling is possible, which would result in changes in the value of T_1 being determined by this process. It is important to stress the difference between the loss of coherence of the free electron motion and the energy relaxation. The first process can be caused by elastic as well as inelastic scattering and is related to the plasmon bandwidth, while the second one is only possible by inelastic scattering processes.

Furthermore, it is unlikely that the phonons have to be excited in order to couple more strongly to the electrons and take up energy through electron−phonon interactions if one considers that the excitation energy of one photon with a wavelength of 520 nm corresponds to 2.38 eV which is distributed among all conduction electrons participating in the coherent excitation. With about 250 000 atoms per particle for the 22 nm size nanoparticles and therefore as many conduction electrons the energy one electron takes up is only 9.5×10^{-6} eV. From the Debye temperature of 170 K for gold[29,30] it follows that all possible phonon modes are already excited at room temperature with the highest excited phonon mode having an energy of 1.5×10^{-2} eV (and greatly exceeding the average excess energy of a single electron). A further temperature increase will therefore have no effect on the available phonon modes with which the electrons can couple.

It can therefore be concluded that it is the population of higher electronic states, which is responsible for a faster dephasing time of the coherent plasmon oscillation and that the dephasing process is thus dominated by the energy spectrum of the electrons and not the phonons. From Fermi liquid theory[40] the electron−electron scattering rate is proportional to the square of the energy difference of the excited state and the Fermi energy E_F.

$$\frac{1}{\tau_{e-e}} \propto (E - E_F)^2 \tag{6}$$

Because the Fermi distribution of the electrons varies only slowly with temperature and the scattering rate depends strongly on the availability of empty states just above or below the Fermi level, it seems very sensible that there is only a small temperature dependence for the plasmon absorption in gold nanoparticles.

Higher electronic temperatures do not only lead to a faster electron−electron scattering rate but should also increase the electron−surface and electron−defect scattering. The velocity of an electron depends on its state energy and therefore on the temperature. It increases for higher excited electronic states. From eq 4 it can be seen that an increase in the velocity of the electrons leads to a larger damping constant γ and therefore to a faster dephasing. A similar explanation was also given in connection with a jellium model approach where the relaxation

dynamics were treated as Landau damping in close analogy to nuclear processes.[41] Furthermore, this result is also consistent with the model of chemical interface damping as the broadening of the plasmon band is related to the overlap between the energy levels of the metal nanoparticle with those of the surface adsorbed molecules.[18,20] An increased temperature of the electron gas will enable a larger fraction of electrons to undergo a charge transfer into the acceptor levels and cause a faster dephasing of the plasmon oscillation.

Electron-defect scattering can however be ruled out as the dominant dephasing mechanism for a different reason. High-resolution TEM studies on these nanoparticles[42] show that the gold nanoparticles contain multiple twins and stacking faults randomly distributed inside these particles. As the larger nanoparticles (48 and 99 nm) are grown from the smaller ones their cores must be structurally identical to the smaller nanoparticles. The random distribution of the defect structures should therefore wash out any size dependence of the plasmon bandwidth if electron−defect scattering was the dominating dephasing process determining T_2.

Another indication that electronic states must be excited for a broadening of the plasmon band are the experiments on the ultrafast bleaching of the plasmon band when heated with a femtosecond laser.[43−49] The observed transient absorption spectrum was shown to be caused by the broadening of the plasmon band after excitation. The temperature rise from the femtosecond laser photothermal heating in these experiments was estimated to be in the range of several hundred to 1000 K. As the transient bleach is observed instantaneously the broadening has to be ascribed to a change in the electron distribution as no equilibration with the lattice has yet taken place. The cooling of the electron gas is mainly caused by electron−phonon scattering and leads to an increase of the lattice temperature but also to the decay of the transient signal on the picosecond time scale.

Our conclusions about the dephasing of the plasmon oscillation are in agreement with a sequence of relaxation time domains in noble metal nanoparticles compiled recently by Kreibig et al.[20] Phase relaxation occurs on the order of 10 fs while electron−electron scattering and electron−phonon energy relaxation is typically on the order of 100 fs and 1 ps, respectively.

Acknowledgment. This work was supported by the Office of Naval Research (through Grant No. N00014-95-1-0306) and the Georgia Tech Molecular Design Institute (through Grant No. N00014-95-1-1116). S.L. thanks the German Fond der Chemischen Industrie and the German BMBF for a Ph.D. fellowship.

References and Notes

(1) Henglein, A. *J. Phys. Chem.* **1993**, *97*, 8457.
(2) Henglein, A. *Chem. Rev.* **1989**, *89*, 1861.
(3) Alivisatos, A. P. *J. Phys. Chem.* **1996**, *100*, 13226.
(4) Schmid, G. *Clusters Colloids: From Theory to Application*; VCH: Weinheim, 1994.
(5) Kreibig, U.; Vollmer, M. *Optical Properties of Metal Clusters*; Springer: Berlin, 1995.
(6) Papavassiliou, G. C. *Prog. Solid State Chem.* **1980**, *12*, 185.
(7) Perenboom, J. A. A. J.; Wyder, P.; Meier, P. *Phys. Rep.* **1981**, *78*, 173.
(8) Hughes, A. E.; Jain, S. C. *Adv. Phys.* **1979**, *28*, 717.
(9) Kerker, M. *The Scattering of Light and Other Electromagnetic Radiation*; Academic Press: New York, 1969.
(10) Bohren, C. F.; Huffman, D. R. *Absorption and Scattering of Light by Small Particles*; Wiley: New York, 1983.
(11) Creighton, J. A.; Eadon, D. G. *J. Chem. Soc., Faraday Trans.* **1991**, *87*, 3881.
(12) Mulvaney, P. *Langmuir* **1996**, *12*, 788.
(13) Brus, L. E. *Appl. Phys. A* **1991**, *53*, 465.
(14) Mie, G. *Ann. Physik* **1908**, *25*, 377.
(15) Kreibig, U.; Genzel, U. *Surf. Sci.* **1985**, *156*, 678.
(16) Kreibig, U.; v. Fragstein, C. *Z. Phys.* **1969**, *224*, 307.
(17) Kawabata, A.; Kubo, R. *J. Phys. Soc. Jpn.* **1966**, *21*, 1765.
(18) Persson, N. J. *Surf. Sci.* **1993**, *281*, 153.
(19) Hoevel, H.; Fritz, S.; Hilger, A.; Kreibig, U.; Vollmer, M. *Phys. Rev. B* **1993**, *48*, 18178.
(20) Kreibig, U.; Gartz, M.; Hilger, A. *Ber. Bunsen-Ges. Phys. Chem.* **1997**, *101*, 1593.
(21) Turkevich, J.; Stevenson, P. C.; Hillier, J. *Discuss. Faraday Soc.* **1951**, *11*, 55.
(22) Turkevich, J.; Garton, G.; Stevenson, P. C. *J. Colloid Sci.* **1954**, Supplement 1, 26.
(23) Turkevich, J. *Gold Bull.* **1985**, *18*, 86.
(24) Handley, D. A. *Colloidal Gold: principles, Methods, and Applications*, Vol. 1; Academic Press: New York, 1989.
(25) Kreibig, U. *J. Phys. F* **1974**, *4*, 999.
(26) Kreibig, U. *Z. Phys. B* **1978**, *31*, 39.
(27) Heilweil, E. J.; Hochstrasser, R. M. *J. Chem. Phys.* **1985**, *82*, 4762.
(28) Alvarez, M. M.; Khoury, J. T.; Schaaff, T. G.; Shafigullin, M. N.; Vezmer, I.; Whetten, R. L. *J. Phys. Chem. B* **1997**, *101*, 3706.
(29) Ashcroft, N. W.; Mermin, N. D. *Solid State Physics*; Saunders College: Philadelphia, 1976.
(30) Kittel, C. *Introduction to Solid State Physics*; Wiley: New York, 1996.
(31) Puech, K.; Henari, F. Z.; Blau, W. J.; Duff, D.; Schmid, G. *Chem. Phys. Lett.* **1995**, *247*, 13.
(32) Lamprecht, B.; Leitner, A.; Aussenegg, F. R. *Appl. Phys. B* **1997**, *64*, 269.
(33) Steinmueller-Nethl, D.; Hoepfel, R. A.; Gornik, E.; Leitner, A.; Aussenegg, F. R. *Phys. Rev. Lett.* **1992**, *68*, 389.
(34) Klar, T.; Perner, M.; Grosse. S.; v. Plessen, G.; Spirkl, W.; Feldmann, J. *Phys. Rev. Lett.* **1998**, *80*, 4249.
(35) Kreibig, U. *J. Phys.* **1977**, *38*, C2−97.
(36) Kreibig, U. *Solid State Commun.* **1978**, *28*, 767.
(37) Doremus, R. H. *J. Chem. Phys.* **1965**, *42*, 414.
(38) Doremus, R. H. *J. Chem. Phys.* **1964**, *40*, 2389.
(39) Turro, N. J. *Modern Molecular Photochemistry*; University Science Books: Mill Valley, 1991.
(40) Pines, D.; Nozieres, P. *The Theory of Quantum Liquids*; Benjamine: New York 1966.
(41) Yannouleas, C.; Broglia, R. A. *Ann. Phys.* **1992**, *217*, 105.
(42) Link, S.; Burda, C.; Wang, Z. L.; El-Sayed, M. A. *J. Chem. Phys.*, submitted.
(43) Ahmadi, T. S.; Logunov, S. L.; El-Sayed, M. A. *J. Phys. Chem.* **1996**, *100*, 8053.
(44) Ahmadi, T. S.; Logunov, S. L.; El-Sayed, M. A.; Khoury, J. T.; Whetten, R. L. *J. Phys. Chem. B* **1997**, *101*, 3713.
(45) Perner, M.; Bost, P.; v. Plessen, G.; Feldmann, J.; Becker, U.; Mennig, M.; Schmidt, H. *Phys. Rev. Lett.* **1997**, *78*, 2192.
(46) Hodak, J. K.; Martini, I.; Hartland, G. V. *J. Phys. Chem. B* **1998**, *102*, 6958.
(47) Hodak, J. K.; Martini, I.; Hartland, G. V. *Chem. Phys. Lett.* **1998**, *284*, 135.
(48) Smith, B. A.; Waters, D. M.; Faulhaber, A. E.; Kreger, M. A.; Roberti, T. W.; Zhang, J. Z. *J. Sol−Gel Sci. Technol.* **1997**, *9*, 125.
(49) Faulhaber, A. E.; Smith, B. A.; Andersen, J. K.; Zhang, J. Z. *Mol. Cryst. Liq. Cryst.* **1996**, *283*, 25.